ELSEVIER

Catalysis Today 50 (1999) 237–245

CATALYSIS TODAY

Carbon deposition in Pd/CeO_2 catalyst: TEM study

Leszek Kępiński*

Institute of Low Temperature and Structure Research, Polish Academy of Sciences, PO Box 1410, 50-950, Wrocław, Poland

Abstract

Morphology and distribution of carbon deposit accumulated in Pd/CeO_2 catalyst, Pd black and Pd_3Ce alloy during heating in ethylene at 873 K was studied by transmission electron microscopy (TEM) and selected area electron diffraction (SAED). In Pd/CeO_2 catalyst filamentous carbon was formed, with microstructure depending strongly on temperature of the catalyst reduction in hydrogen. Samples reduced at 673 and 773 K produced filaments exhibiting ''whisker-like'' mode of growth (metal particles were located at the tip of the filaments), while those reduced at 973 and 1100 K produced ''extrusion-like'' filaments (Pd particles were located at the bottom, attached to ceria crystallites). Reduction of the Pd/CeO_2 catalyst at 1200 K hindered completely the formation of carbon filaments. Extensive carbon deposit in the form of whiskers and shells occurred in Pd black, while no carbon deposition was observed in Pd_3Ce alloy.

The change in the filament growth mode with increasing temperature of reduction has been explained by increasing strength of the Pd–ceria interaction (epitaxial orientation of Pd particles on CeO_2, decoration of Pd surface with partly reduced ceria species and formation of Pd–Ce alloy).

Keywords: Pd/CeO_2 catalyst; Palladium on ceria; Carbon filaments; Metal–oxide interaction; Coking

1. Introduction

An important problem in the catalytic processing of carbon-containing feeds is the deposition of carbon. Among several forms of carbon deposits differing in morphology, reactivity, and therefore, influence on the catalytic performance there is one, filamentous carbon, which attracted particular attention due to its very interesting physical properties on the one hand, and its detrimental action on the catalyst on the other hand [1]. Transition metals used as the catalysts in hydrocarbons processing are also very active in catalytic formation of carbon filaments at temperatures above 770 K. Recently, it has been found that these metals are also active catalysts of nanotubes formation during carbon evaporation in arc [2].

Process of the filaments growth catalysed by metal particles can be seriously affected by the addition of another element to the metal [3] or by induction of its strong interaction with the support [4,5]. We have shown previously that for Pd and Ni supported on SiO_2 and Al_2O_3 reduction at temperatures above 970 K caused chemical reaction between metal and oxide with the formation of Me–Si or Me–Al alloys which hindered the carbon deposition [6–8]. Since we have found recently that similar effect of alloying occurs in Pd/CeO_2 catalyst reduced at high temperatures [9,10], it was interesting to find out how it influences the process of carbon deposition.

*Fax: +48-71-441029; e-mail: kepinski@int.pan.wroc.pl

0920-5861/99/$ – see front matter
PII: S0920-5861(98)00506-9

2. Experimental

Pd/CeO_2 catalyst (metal loading 3 wt%) was prepared by multiple (three times) impregnation of CeO_2 support with an aqueous solution of Pd nitrate. The ceria support was obtained by slow evaporation at 353 K and then calcination at 623 K for 20 h of 20 wt% colloidal dispersion of CeO_2 in diluted acetic acid (Aldrich). An average crystallite size of the ceria support obtained from XRD line broadening was L_{av}=7 nm, from which a rough estimation of a surface area of 120 m^2/g could be made (S (m^2/g)=6000/(L_{av} (nm)×ρ (g/cm^3)), where ρ=7.14 (g/cm^3) – density of CeO_2). Reduction and carbonization of the Pd/CeO_2 samples were performed in a system that allowed for evacuation of the sample to below 10^{-3} Pa. This enabled efficient removal of hydrogen from Pd (decomposition of Pd hydride that could form during reduction in hydrogen). Reduction was conducted in hydrogen flow (slight overpressure) at temperatures 673–1200 K for 20 h. Then hydrogen was pumped off with the sample kept at the reduction temperature until pressure dropped to 10^{-3} Pa. Finally, temperature was set to 873 K and ethylene was admitted into the system through the leak valve, so that the constant pressure (p=667 Pa) was established. After 1 h ethylene was pumped off and the sample was cooled in vacuum to room temperature. Commercial grade hydrogen was purified by passing it over Pd/asbestos, KOH and P_2O_5. Ethylene (Messer Griesheim – 99.5%) was used as supplied. Microstructure of the samples was investigated with Philips CM20 SuperTwin microscope operated at 200 kV and providing 0.25 nm resolution. Specimens for TEM were prepared by dipping a Cu microscope grid covered with holey carbon into freshly ground sample. Overall structure of the samples was controlled with powder XRD.

As the reference we used palladium black and Pd–Ce alloy containing 25 at% Ce (Pd_3Ce).

The Pd_3Ce alloy was prepared by arc melting the stoichiometric amounts of the constituent elements in a titanium-gettered argon atmosphere. To improve homogeneity the sample was turned over and remelted. The weight losses after meltings were negligible.

Before carbonization a piece of the Pd_3Ce sample was powered by grinding in a mortar in air and then immediately transferred into the vacuum system to minimize possible oxidation. No "in situ" treatment of the alloy was applied before its carbonization in ethylene at 873 K for 1 h.

3. Results

3.1. Pd black

Fig. 1(a) shows a low magnification micrograph of the carburized Pd black. It is seen that Pd is quite an effective catalyst of carbon filaments formation. Wide range of filament sizes and shapes are observed from thin tube-like objects with dia. 5–150 nm exhibiting very high length/diameter ratio to thick, short worn-like objects with low l/d ratio. In addition to carbon

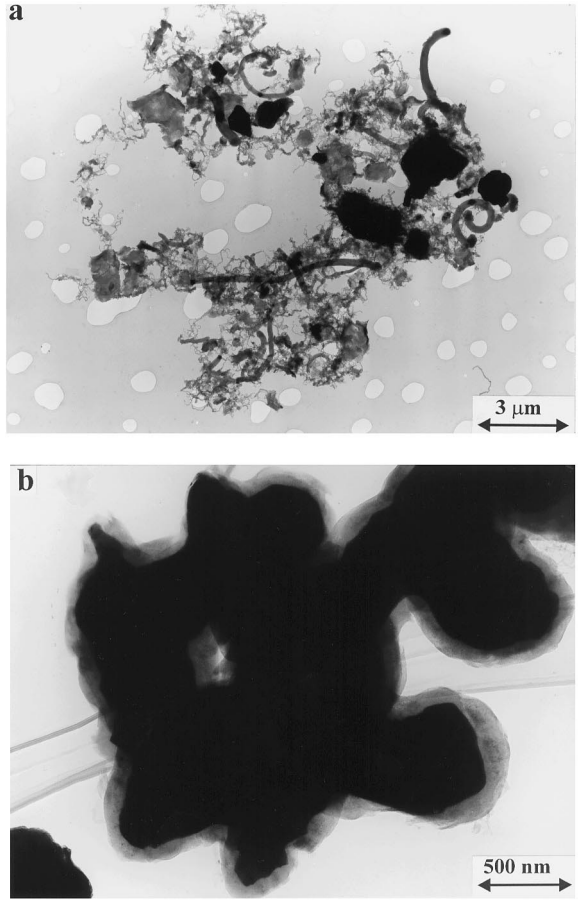

Fig. 1. Morphology of Pd black carburized in ethylene at 873 K. Carbon filaments (a) and carbon shells (b).

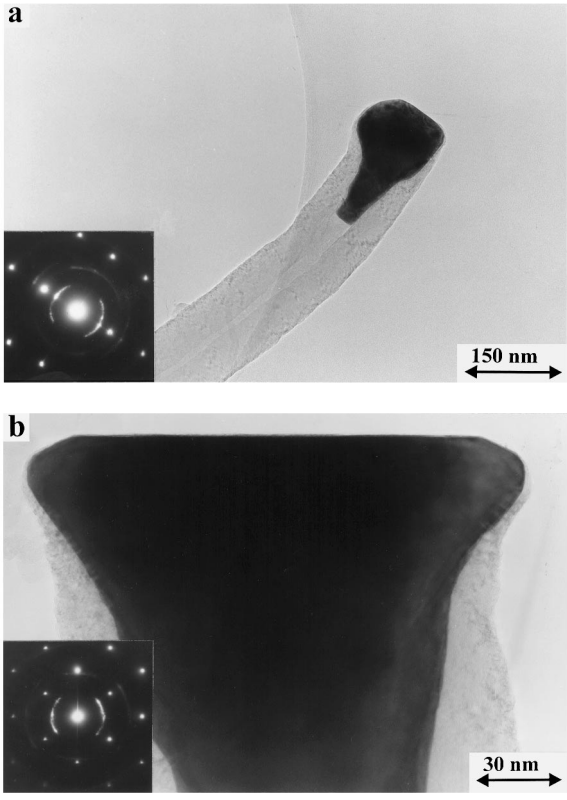

Fig. 2. Microstructure of 'whisker-like' carbon filaments formed in Pd black. Front face of the Pd particles expose (1 1 0) plane (a) and (1 0 0) plane (b). SAED patterns of the Pd particles are shown as insets.

filaments, also large Pd grains covered with thick (∼100 nm) graphite shells are frequently met in the sample (Fig. 1(b)). At higher magnification (Fig. 2) it is seen that the filaments contain the metal particle at the tip with size close to the diameter of the filament indicating whisker-like mode of growth [11]. Shape of the particle is pear-like with well-developed crystal faces. By using selected area electron diffraction (SAED) we were able to determine the exact orientation of the particle in relation to the filament axis and to index the particle faces. It appeared that the front face of the particle exhibits (1 0 0) or (1 1 0) planes. Fig. 2(a) shows an image and SAED pattern of a 'whisker-like' filament oriented with Pd[1 1 2] parallel to the electron beam (see inset). Filament axis is parallel to Pd[1 1 0] and front (carbon free) face of Pd exposes (1 1 0) plane. From SAED pattern it is seen that graphitic planes are roughly parallel to Pd[1 1 1] planes. Fig. 2(b) shows an image and SAED pattern (inset) of another whisker-like filament with Pd particle oriented with [0 1 1] direction parallel to the electron beam. Axis of the filament is parallel to Pd[1 0 0] direction and front face of the particle exposing (1 0 0) plane is free of carbon. At higher magnification it is seen that wall of the filament is composed of well-ordered graphitic planes parallel to the filament axis.

XRD spectra of the carburized Pd black contained only reflections corresponding to Pd (a=0.39 nm).

3.2. Pd/CeO_2

Figs. 3–6 show TEM images of Pd/CeO_2 catalyst carburized in ethylene, after previous reduction in hydrogen at various temperatures. In samples reduced at 673 and 773 K (Fig. 3) Pd particles catalysed filament growth via typical 'whisker' mode, i.e., the particle is situated at the tip of the filament. The filaments have dia. ca. 10 nm, much larger than the diameter of the metal particles. In the body of the filaments there are often dark inclusions which were

Fig. 3. Microstructure of carbon filaments in Pd/CeO_2 sample reduced at 673 or 773 K.

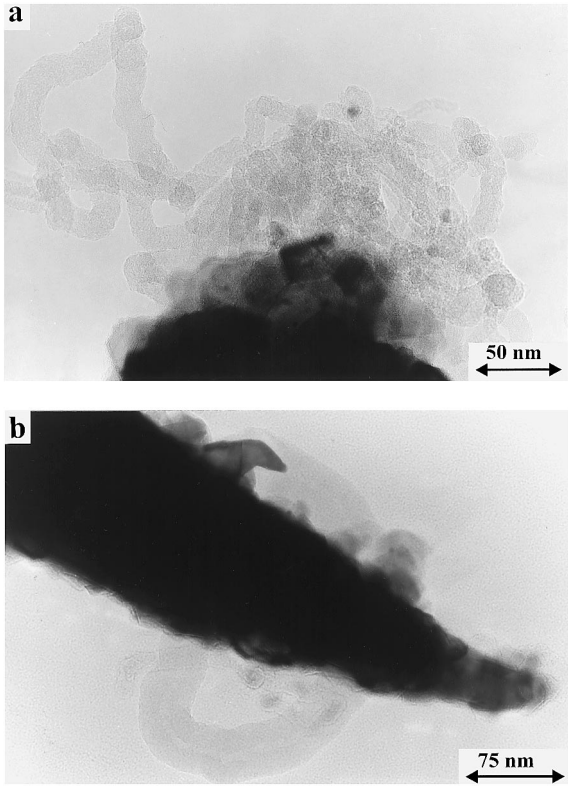

Fig. 4. Microstructure of carbon filaments in Pd/CeO_2 sample reduced at 973 K. Thin, disordered filaments (a), 'extrusion-like' filament (b) and ordering of graphitic layers in 'extrusion-like' filament (c).

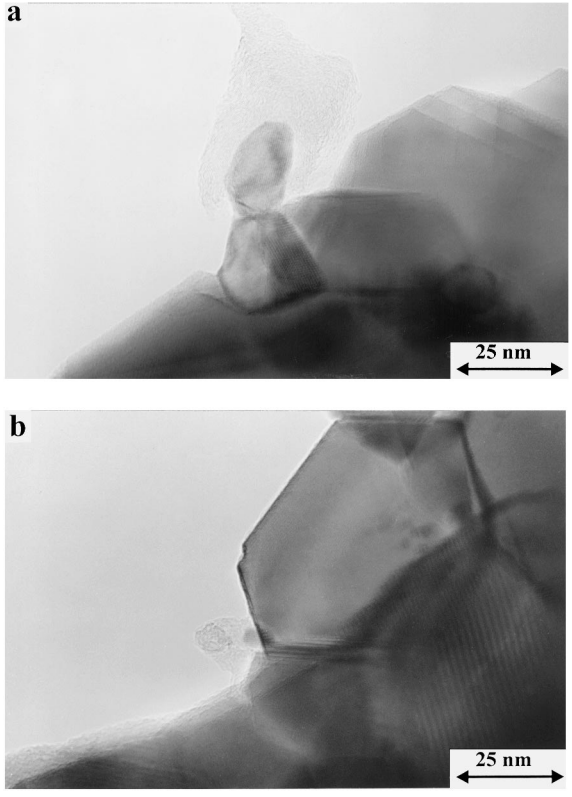

Fig. 5. Carbon deposit in Pd/CeO_2 sample reduced at 1100 K. Note the 'extrusion'-type mode of the filament growth and their highly disordered structure. Moire fringes (~0.8 nm) on Pd particle in (b) indicate epitaxial Pd[1 1 1]||CeO_2[1 1 1] orientation.

identified as palladium. Carbon forming the filament body is poorly ordered with graphitic planes being curled and generally not parallel to the filament axis. Pd particles exhibit irregular, usually oblate shapes with no distinct crystal faces developed.

When reduction temperature increases to 973 K there are still numerous filaments with dia. 15–25 nm and up to 750 nm long, but in most cases Pd particle is now at the bottom of the filaments, attached to ceria crystal (Fig. 4(a)). Pd inclusions within the filaments are very rare. Due to noticeable sintering of palladium at this temperature in the sample there are also particles with larger size (ca. 40 nm) exhibiting characteristic cone-like shape capable to produce tubular carbon filaments (Fig. 4(b)). Ordering of carbon in such filaments is better than in those formed by for smallest particles in Pd/CeO_2 sample. Nevertheless, graphitic planes are bent and the internal channel

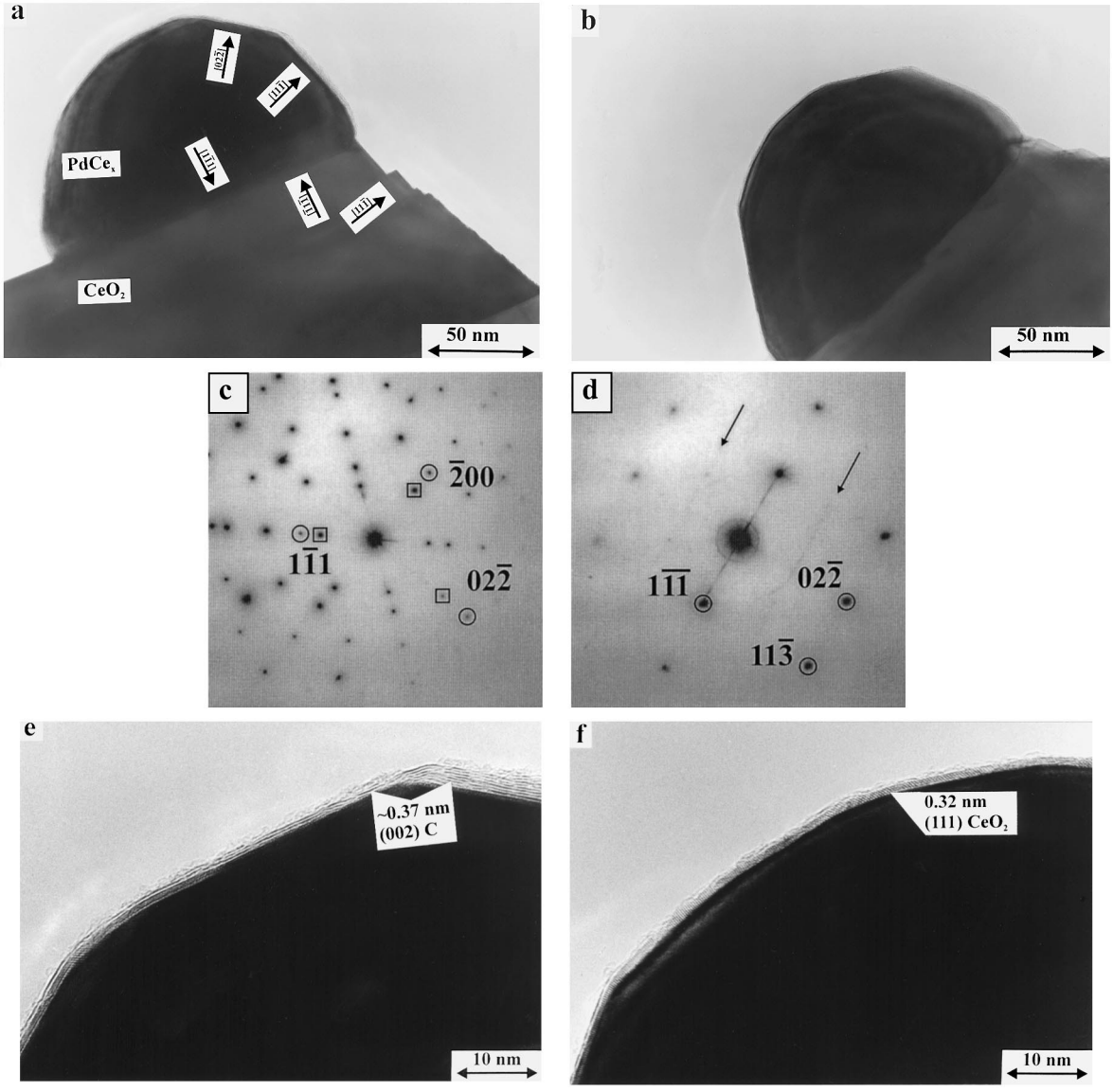

Fig. 6. TEM images and SAED patterns of an inactive Pd particle epitaxially oriented on CeO_2 crystal (sample reduced at 1200 K). [0 1 1] orientation (a), (c) and (e), [2 1 1] orientation (b), (d) and (f). In SAED patterns □ and ○ denote CeO_2 and Pd reflections, respectively.

is divided into compartments (Fig. 4(c)). The morphology of the filaments resembles a bamboo-like structure reported by Saito [2]. Further increase of the reduction temperature to 1100 K changes drastically the number and morphology of the filaments. They are now short, highly disordered with an internal channel poorly visible (Fig. 5(a)). Pd particles on which they grow are always located at the bottom affixed to the support. Small Pd particle in Fig. 5(b) is epitaxially oriented on CeO_2 crystallite with [1 1 1] Pd‖[1 1 1] CeO_2. This orientation causes the appearance of 0.8 nm Moire fringes visible in the image.

In sample reduced at 1200 K the growth of carbon filaments ceases completely. As an example Pd crystallite epitaxially oriented on CeO_2 crystal is shown in Fig. 6. In Fig. 6(a) both Pd and CeO_2 crystallites are

oriented with [0 1 1] direction parallel to the electron beam and with [1 0 0] Pd ‖ [1 0 0] CeO_2 (see SAED pattern in Fig. 6(c)). The Pd–CeO_2 interface is perpendicular to [1 1 1]. Lattice parameter of Pd calculated from SAED is 0.23 nm, i.e. is expanded by ca. 2.3% relative to pure Pd. It is seen that CeO_2 crystal is faceted and exhibits well-developed, clean faces of {1 1 1} type. The Pd particle is also well-crystallized exposing low index planes. In the magnified image (Fig. 6(e)) it is seen that the surface of the particle is covered with an overlayer of nonuniform thickness. At the Pd(1 1 1) face the overlayer is up to 3 nm thick and contains slightly bent 0.37–0.42 nm fringes roughly parallel to the Pd(1 1 1) surface, while at the other faces it is less then 1 nm thick and contains 0.32 nm fringes roughly perpendicular to the surface. In Fig. 6(b) the same Pd particle is shown in orientation close to [2 1 1]. In SAED pattern taken from the metal particle only (Fig. 6(d)) streaks are visible at positions of forbidden Pd 1 1 0 type reflections. This may indicate that the particle consists of a partly ordered Pd–Ce alloy. In the magnified image (Fig. 6(f)) an ordered, 0.9 nm overlayer exhibiting 0.32 nm fringes is clearly visible.

For all Pd/CeO_2 samples subjected to carbonization deposition of carbon occurs exclusively at Pd particles with ceria crystallites being practically free of carbon (in some cases thin, amorphous carbon layer covering entire surface of the sample was seen, but it resulted from the contamination inside the microscope).

Evolution of the overall structure of the catalyst sample as studied by XRD was consistent with previously reported schemes [9,10,12]. At temperature of reduction 973 and 1100 K ceria support was transformed to pseudo cubic CeO_{2-x} phase exhibiting expanded lattice parameter, but at 1200 K partial reduction to hexagonal Ce_2O_3 took place. Growth of an average size of the ceria crystallites with increasing temperature of reduction deduced from XRD L_{av}=18, 28 and 30 nm for 673, 973 and 1100 K, respectively, indicated sintering of the support and therefore decrease of its surface area (to 47, 30 and 28 m^2/g, respectively). Obviously, the value for the surface area obtained for severely sintered sample (973 and 110 K) overestimate the ''true'' BET surface area because significant fraction of crystallites is in fact not accessible for the gas adsorption [13]. Due to low metal loading and small size of crystallites Pd reflections could not be observed in XRD spectra, except for the highest reduction temperature (1200 K), where weak Pd 1 1 1 peak was detected at 2Θ=39.28° (Cu K_α radiation) corresponding to expanded Pd lattice parameter (a=0.397 nm).

3.3. Pd–Ce alloy

In Fig. 7(a) a low magnification image of large crystal in carburized Pd_3Ce sample is shown. SAED pattern (Fig. 7(c)) allowed us to identify it as cubic Pd_3Ce (Pm3m space group, a=0.413 nm in good agreement with literature data [14]) oriented with [1 1 1] direction parallel to the electron beam. Note that the mixed odd–even reflections are easily observable in SAED pattern, though these are hardly visible in XRD spectrum. Part of the crystal imaged at high magnification is shown in Fig. 7(b). Obviously, there is no indication of any noticeable carbon deposition on the surface of the crystal. This behaviour is in contrast to that of Pd black carburized at the same conditions, where thick graphite shell is formed on the surface of large particles (cf. Fig. 1(b)).

4. Discussion

Our results show that Pd particles with broad range of sizes (2–50 nm) both unsupported as well as supported on CeO_2 catalyse the formation of filamentous carbon from ethylene at 873 K. Growth of carbon filaments with similar morphology from acetylene or ethylene in Pd/C at 920 K [15] and in Pd/SiO_2 at 770 K [16] has already been reported in the literature.

Microstructure of the filaments formed on Pd black (Figs. 1 and 2) is characteristic for the so-called 'whisker-like' growth type [11]. They are tubes of uniform diameter containing well-crystallised metal particle at the tip. Diameter of the filament is equal to that of the particle (Fig. 2). Growth of such filaments catalysed by various transition metals (mainly Fe, Co, Ni) and their alloys was described in numerous papers (see e.g. [17] and references therein), and the mechanism of the growth process is well-established [18]. In general, the process involves the following steps: formation of atomic carbon on the front face of metal particle by decomposition of hydrocarbon molecules, dissolution of these carbon atoms into the metal

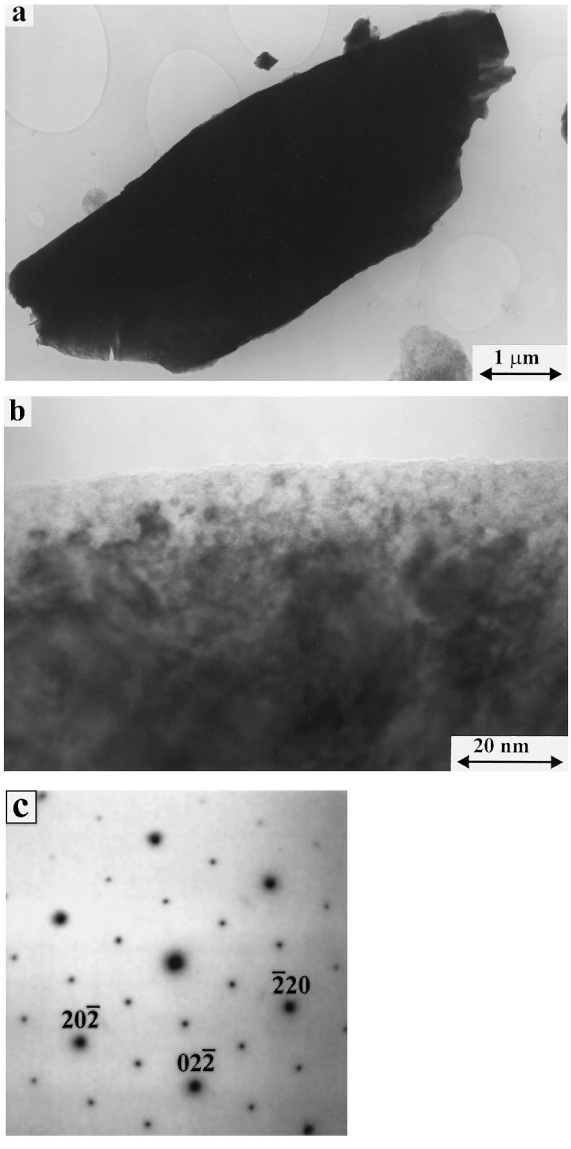

Fig. 7. Low (a) and high magnification (b) images of a crystal in Pd_3Ce sample carburized at 873 K. SAED pattern of the crystal indicating [1 1 1] orientation (c).

particle, diffusion of carbon atoms to the rear and then precipitation as graphitic layers. A necessary step to initiate a steady-state growth of the filament is the reconstruction and faceting of the metal particle [18]. We assume that due to clear similarities in morphology this mechanism operates also for palladium. Crystallographically rough (1 0 0) and (1 1 0) facets act as places active in ethylene decomposition, while "flat" (1 1 1) planes at the rear are places for graphite precipitation. UHV studies on metal single-crystal surfaces showed that on Pd(1 1 0) [19] and Pt(1 1 0) and (1 0 0) [20] ethylene decomposes upon heating to form reactive carbon species with no C–C bonds present. On the contrary, graphitic carbon (with C–C bonds) is formed on Pt(1 1 1) surface under similar conditions [21].

For Pd particles supported on CeO_2 we also observed growth of carbon filaments (Fig. 3), however their morphology is different. For samples reduced at 673 and 773 K carbon forming filaments body is highly disordered. Pd particles exhibit irregular shapes with no distinct faces developed and are located not only at the tip but also inside the filaments. Such morphology is identical to that reported by Zaikovskii et al. [22] for Ni catalysed filament growth. The authors ascribed this particular morphology of the filaments to the size effect (Ni particles with size below ca. 10 nm behaves in this way, while those larger than 10–20 nm produced regular well ordered whisker-like filaments). Occurrence of the metal particles inside the filaments is probably the results of defragmentation of the original catalytic particle during the filament growth. We agree with Zaikovskii et al. [22] that possible cause of the rapture is accumulation of carbon at the intergranular boundaries inside polycrystalline Pd aggregate. Such aggregates are likely to form during the preparation of the Pd/CeO_2 catalyst.

When temperature of reduction increases to 973 K morphology of the filaments changes. Extensive sintering of Pd which occurs at this temperature [9,10], creates Pd particles with sizes above 20 nm able to catalyse well-defined tubular filaments (Fig. 4(b) and (c)). Concurrently, reduction of Pd/CeO_2 at 973 K is known to induce strong bonding between Pd and ceria [9,10], so that the Pd particles cannot be lifted up from the support and the filaments grow in 'extrusion mode' (with metal particle at the bottom) (Fig. 4(b)). This mode of growth has been reported by Baker [11] for ruthenium on graphite and on silica. Further increase of the reduction temperature causes gradual loss of the activity of Pd particles in filaments formation till its complete termination at 1200 K.

Three phenomena occurring during high temperature reduction of Pd/CeO_2 catalyst may effect the process of the filamentous carbon growth. These

are: epitaxial orientation of Pd particles on CeO_2 surface, decoration of Pd surface with partly reduced ceria species and an interfacial reaction between Pd and ceria leading to the formation of Pd–Ce alloy. Preferential, epitaxial orientation of Pd particles on CeO_2 surface occurs on reduction at 973 K [9] and has been observed for other metals on CeO_2: Rh [23,24] at 623 K and Pt [25–27] at 773–973 K. Formation of an ordered Me–CeO_2 phase boundary lowers the interfacial energy and thus increases the Me–CeO_2 bonding. We believe that this effect is responsible for the observed change of the mode of filament growth from the whisker-like to extrusion-like.

Decoration of the surface of Pd particles with ceria species evidenced in Fig. 6(e) and (f) was already reported for Pd at 673–973 K [9,10,28,29] and for Rh [23] and Pt [25] at 973 K. It should be mentioned that the statement in [29] that Ce_2O_3 is formed during reduction at unexpectedly low temperature (773 K) and migrates over Pd was based on the misinterpretation of the XRD spectrum. In fact the authors observed tetragonal CeOCl phase, which is very stable in reducing atmosphere [10]. Presence of patches of CeO_x on Pd decreases the active surface available for ethylene decomposition and for the formation of well-ordered graphitic planes. As the result short, highly disordered filaments are observed in the sample reduced above 973 K.

Formation of Pd–Ce alloy in Pd/CeO_2 reduced at 1200 K may be deduced from the presence of the forbidden reflections in the SAED pattern (Fig. 6(c)) and from the shift of Pd 1 1 1 peak in XRD spectrum. This latter effect was studied thoroughly in our previous works [9,10]. Recently, Bernal at al. [25] presented HRTEM micrographs of an ordered Pt_5Ce compound formed in Pt/CeO_2 catalyst reduced at 1073 K. These facts together with the observation that Pd_3Ce is inactive in process of carbon formation (Fig. 7) allow us to assume that complete loss of the activity of Pd in filament growth observed after reduction at 1200 K is caused by simultaneous occurrence of the two processes: formation of a bulk Pd–Ce alloy and decoration of the surface of the particles with the ceria overlayer. The ceria overlayer blocks the surface available for the gas decomposition, while the presence of Ce atoms in Pd lattice lowers the solubility of carbon in Pd and thus terminates one necessary step in the process of filament growth. Existing data show that hydrogen solubility in Pd decreases to nearly zero for Ce content in Pd of about 8 at% [30,31]. Since hydrogen and carbon occupy the same sites in the Pd lattice [32] we may expect similar behaviour for carbon. In earlier papers we have shown also that introduction of Si into Pd [16] or Ni [6] hinders the growth of filamentous carbon and the role of Si is to retard the rate of carbon solubility and diffusivity in the metal. It could be argued that an apparent inactivity of Pd_3Ce in the carbon formation reported in this work is not an intrinsic property of the alloy but is rather caused by oxidation of its surface during grinding in air. Obviously we cannot exclude such effect, but we assume that only thin and poorly ordered oxide layer may be formed (no distinct CeO_2 reflections in Fig. 7(b)). Such a layer is, however, unlikely to isolate completely Pd_3Ce surface from the ethylene atmosphere and other mechanism (as this described above) must determine the carbon formation. Baker and Chludzinski [33] showed that oxide overlayers on the surface of Ni–Fe surface only to some extend hinderes the formation of filamentous carbon from acetylene, while incorporation of the additive into the catalyst totally blocks the filament growth.

Acknowledgements

The author thanks Mrs. M. Koźlik for the preparation of Pd_3Ce alloy, Mrs. M. Razik for performing XRD analysis and Mrs. Z. Mazurkiewicz for the valuable technical assistance in the experiments.

References

[1] J.R. Rostrup-Nielsen, Catalytic steam reforming, in: Catalysis, Science and Technology, vol. 5, Springer, Berlin, 1984, p. 1.
[2] Y. Saito, Carbon 33 (1995) 979.
[3] C. Park, N.M. Rodriguez, R.T.K. Baker, J.Catal. 169 (1997) 212.
[4] C.H. Bartholomew, M.V. Strasburg, H.Y. Hsieh, Appl. Catal. 36 (1988) 147.
[5] E.T.C. Vogt, A.J. van Dillem, J. Geus, in: B. Delmon, C.F. Froment (Eds.), Catalyst Deactivation, 1987, Elsevier, Amsterdam, 1987, p. 221.
[6] Kępiński, L., Carbon 30 (1992) 949.
[7] Kępiński, L.M. Wołcyrz, Appl. Catal. 73 (1991) 173.
[8] Kępiński, L.M. Wołcyrz, J. Jabłoński, Appl. Catal. 54 (1989) 267.

[9] Kępiński, L.M. Wołcyrz, Appl. Catal. 150 (1997) 197.
[10] Kępiński, L.M. Wołcyrz, J. Okal, J. Chem. Soc., Faraday Trans. 91 (1995) 507.
[11] R.T.K. Baker, Carbon 27 (1989) 315.
[12] V. Perrichon, A. Laachir, G. Bergeret, R. Frety, L. Tournayan, O. Touret, J. Chem. Soc., Faraday Trans. 90 (1994) 773.
[13] V. Perrichon, A. Laachir, S. Abouarnadasse, O. Touret, G. Blanchard, Appl. Catal. A 129 (1995) 69.
[14] Y. Sakamoto, K. Takao, M. Ohmaki, J. Less-Common Met. 162 (1990) 343.
[15] R.T.K. Baker, J.A. France, J. Catal. 39 (1975) 481.
[16] Kępiński, L., React. Kinet. Catal. Lett. 38 (1989) 363.
[17] E. Tracz, R. Scholz, T. Borowiecki, Appl. Catal. 66 (1990) 133.
[18] J.W. Snoeck, G.F. Froment, M. Flowles, J. Catal. 169 (1997) 240.
[19] M. Nishijima, J. Yoshinobu, T. Sekitami, M. Onchi, J. Chem. Phys. 90 (1989) 5114.
[20] R.I. Kvon, A.I. Boronin, Sh.K. Shaikhutdinov, R.A. Buyanov, Appl. Surf. Sci. 120 (1997) 239.
[21] M. Abon, J. Billy, J.C. Bertolini, B. Tardy, Surf. Sci. 150 (1986) 1.
[22] V.I. Zaikovskii, V.V. Chesnakov, R.A. Buyanov, Appl. Catal. 38 (1988) 41.
[23] S. Bernal, F.J. Botana, J.J. Calvino, G.A. Cifredo, J.A. Perez-Omil, J.M. Pintado, Catal. Today 23 (1995) 219.
[24] M. Pan, J.M. Cowley, R. Garcia, Micron. Microsc. Acta 18 (1987) 165.
[25] S. Bernal, J.J. Calvino, J.M. Gatica, C. Larese, C. Lopez-Cartes, J.A. Perez-Omil, J. Catal. 169 (1997) 510.
[26] H.D. Cochrane, J.L. Hutchison, D. White, G.M. Parkinson, C. Dupas, A.J. Scott, Ultramicroscopy 34 (1990) 10.
[27] A.K. Dayte, D.S. Kalakkad, M.H. Yao, J. Smith, J. Catal. 155 (1995) 148.
[28] A. Badri, C. Binet, J.C. Lavalley, J. Chem. Soc., Faraday Trans. 92 (1996) 1603.
[29] L. Fan, K. Fujimoto, J. Catal. 150 (1994) 217.
[30] J. Evans, I.R. Harris, P.F. Martin, J. Less-Common Met. 75 (1980) 49.
[31] Y. Sakamoto, K. Yuwasa, K. Hirayama, J. Less-Common Met. 88 (1982) 115.
[32] S.B. Ziemecki, Reactivity of Solids 1 (1986) 195.
[33] R.T.K. Baker, J.J. Chludzinski, J. Catal. 64 (1980) 464.